Water Research 224 (2022) 119070

Contents lists available at ScienceDirect

Water Research

journal homepage: www.elsevier.com/locate/watres

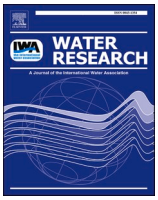

Biofilm-responsive encapsulated-phage coating for autonomous biofouling mitigation in water storage systems

Pengxiao Zuo [a,d], Jordin Metz [b,d], Pingfeng Yu [c], Pedro J.J. Alvarez [a,b,d,*]

[a] Department of Civil and Environmental Engineering, Rice University, Houston, USA
[b] Department of Chemistry, Rice University, Houston, USA
[c] College of Environmental and Resource Sciences, Zhejiang University, Hangzhou, China
[d] Nanosystems Engineering Research Center for Nanotechnology-Enabled Water Treatment, USA

ARTICLE INFO

Keywords:
pH-Responsive
Controlled release
Biofilm control
Crosslinked chitosan
Plasma treatment
Biopolymer

ABSTRACT

Biofilms in water storage systems may harbor pathogens that threaten public health. Chemical disinfectants are marginally effective in eradicating biofilms due to limited penetration, and often generate harmful disinfection byproducts. To enhance biofouling mitigation in household water storage tanks, we encapsulated bacteriophages (phages) in chitosan crosslinked with tri-polyphosphate and 3-glycidoxypropyltrimethoxysilane. Phages served as self-propagating green biocides that exclusively infect bacteria. This pH-responsive encapsulation (244 ± 11 nm) enabled autonomous release of phages in response to acidic pH associated with biofilms (corroborated by confocal microscopy with pH-indicator dye SNARF-4F), but otherwise remained stable in pH-neutral tap water for one month. Encapsulated phages instantly bind to plasma-treated plastic and fiberglass surfaces, providing a facile coating method that protects surfaces highly vulnerable to biofouling. Biofilm formation assays were conducted in tap water amended with 200 mg/L glucose to accelerate growth and attachment of *Pseudomonas aeruginosa*, an opportunistic pathogen commonly associated with biofilms in drinking water distribution and storage systems. Biofilms formation on plastic surfaces coated with encapsulated phages decreased to only 6.7 ± 0.2% (on a biomass basis) relative to the uncoated controls. Likewise, biofilm surface area coverage (4.8 ± 0.2 log CFU/mm^2) and live/dead fluorescence ratio (1.80) were also lower than the controls (6.6 ± 0.2 log CFU/mm^2 and live/dead ratio of 11.05). Overall, this study offers proof-of-concept of a chemical-free, easily implementable approach to control problematic biofilm-dwelling bacteria and highlights benefits of this bottom-up biofouling control approach that obviates the challenge of poor biofilm penetration by biocides.

1. Introduction

Biofilms are the preferred lifestyle for most bacteria, including those present in drinking water treatment, distribution, and storage systems (Flemming and Wuertz, 2019). This poses significant challenges for public and infrastructure health, since biofilms may harbor pathogenic bacteria and promote biofouling and corrosion (Flemming et al., 2016). Biofilms are notoriously difficult to eradicate due to limited penetration by chemical disinfectants, which incidentally may produce harmful disinfection byproducts (DBPs) (Bridier et al., 2011). Mechanical approaches are occasionally used to remove biofilms, but these work only for accessible surfaces (which is not the case for much of the water infrastructure) and are generally energy intensive. Thus, there is a need for alternative chemical-free, eco-friendly approaches to mitigate biofilm formation.

Bacteriophages (phages) are "green biocides" that can exclusively and selectively target pathogenic and other problematic bacteria strains without producing harmful disinfection byproducts (de Jonge et al., 2019; Hicks et al., 2020). Due to their biological nature, phages can self-propagate exponentially, resulting in cost effective bactericidal capacity even with low initial dosage (Yu et al., 2019). This self-propagating nature also makes phage production easily scalable and relatively inexpensive (Anam et al., 2020; Luong et al., 2020). Thus, phage technology could be suitable for some resource-limited areas with infrastructure limitations hindering conventional biocontrol approaches. Phages can also work synergistically with other biofilm control approaches to supplement current treatment methods and curtail chemical use (Stachler et al., 2021).

* Corresponding author at: Department of Civil and Environmental Engineering, Rice University, Houston, USA.
E-mail address: alvarez@rice.edu (P.J.J. Alvarez).

https://doi.org/10.1016/j.watres.2022.119070
Received 19 May 2022; Received in revised form 26 August 2022; Accepted 5 September 2022
Available online 7 September 2022

Encapsulation technology, which is commonly used to protect medicinal drugs and other therapeutics from degradation and enable targeted release at desired locations, may offer opportunities to mitigate biofilm formation by theoretically facilitating on-demand, autonomous release of phages triggered by the presence of bacteria (Herrera et al., 2021). Current technology is focused on oral drug delivery to the intestines using a pH-responsive encapsulation that is stable at low pH but releases the contents at slightly basic pH. These encapsulations protect the medical drug cargo from degradation in the low pH of the stomach and enables controlled release in the slightly basic pH of the intestines (Centurion et al., 2021; Du et al., 2015; Liu et al., 2017). This drug encapsulation technology for targeted delivery is underutilized outside of medicine. By reversing the pH responsiveness of these encapsulations to protect the cargo at the slightly basic pH of tap water and release it into the acidic pH of biofilms, which was demonstrated to be possible for chemical compounds (Chen et al., 2018), we could mitigate wasteful release of phages and target where nascent biofilms form with greater precision.

Note that two major limitations of using free phages for biofilm control is the general lack of targeted delivery to where biofilms form, and poor penetration into the biofilm. Thus, encapsulation technology, which has been used for targeted delivery of chemical compounds to biofilms (Peng et al., 2021), shows promise for enabling targeted delivery of phages to nascent biofilms. Accordingly, we envision a system for encapsulating various phages (which could be switched out and rotated as needed to ensure the phages are fit for purpose) as coatings to selectively protect vulnerable surfaces and attack biofilms from the bottom-up to circumvent poor penetration from the top. This approach would serve as an alternative or supplement to chemical disinfectants, which bluntly target bacteria in the bulk volume of water storage systems.

In this study, we demonstrate an autonomous bottom-up approach to mitigate nascent biofilms using an encapsulated phage coating. A phage isolated from wastewater as previously described (Yu et al., 2019) was used against the opportunistic pathogen *Pseudomonas aeruginosa*, a common biofilm-forming bacterium prevalent in water distribution and storage systems (Chao et al., 2015; Tanner et al., 2019). Additionally, *Pseudomonas* spp. are early colonizers that facilitate subsequent attachment by other bacterial species in chlorinated drinking water distribution systems (Douterelo et al., 2014; Liu et al., 2016) and commonly harbor antibiotic resistance genes, making them an important target for biocontrol (Haller et al., 2018; Mortimer et al., 2018). Phages were encapsulated in a responsive coating made of chitosan crosslinked with tri-polyphosphate (TPP) and 3-glycidoxypropyltrimethoxysilane (GPTMS). We examined the long-term stability and efficacy of the encapsulated phages to mitigate biofilm formation in tap water storage systems. A facile coating process was developed to attach the encapsulated phages to surfaces where biofilm formation is most likely to occur (e.g., bottom of water storage tanks that are commonly used by households in resource-limited areas). Overall, we offer proof-of-concept that autonomous release of bactericidal phages from their encapsulation (triggered by the presence of bacteria) acts as a preventative treatment against biofilm formation to mitigate bacterial reservoirs that could cause water-borne infectious diseases.

2. Experimental methods

2.1. Materials

Acetic acid, sodium hydroxide (NaOH), and hydrochloric acid (HCl) were purchased from Sigma-Aldrich. The chitosan used in this study was 85% deacetylated and purchased from Thermo Fisher. Sodium tripolyphosphate (TPP) (85% pure) was from Acros Organics and 3-glycidoxypropyltrimethoxysilane (GPTMS) (97% pure) was from Tokyo Chemical Industry. Solutions were prepared in deionized water (DI). For biofilm viability assays, SYTO 9 (5mM stock) was from Invitrogen and propidium iodide (20 mM) was from Sigma-Aldrich. Phosphate buffered solution (PBS) was made using PBS tablets from VWR Life Science. SNARF-4F 5-(and-6)-carboxylic acid was obtained from Thermo Fisher for biofilm pH measurements (Hunter and Beveridge, 2005; Schlafer et al., 2015).

Pseudomonas aeruginosa PAO1 (ATCC 15692) was cultured in tryptic soy broth (TSB) (BD Difco) at 30°C. The phage PEB2 used in this study infecting *P. aeruginosa* PAO1 was isolated from wastewater as previously described and characterized to be around 86 nm (Yu et al., 2019). Phage stocks were suspended in sulfate magnesium (SM) buffer as previously described and stored at 4°C (Zuo et al., 2021). Double-layer plaque assays were done using a base layer of dextrose BD Difco plate count agar, and a top layer of tryptic soy agar (0.3% wt/vol agar).

2.2. Encapsulating phages in crosslinked chitosan nanospheres

Under continuous magnetic stirring at room temperature, 5 mg/ml of chitosan was dissolved into a 2% v/v acetic acid aqueous solution. Then, the pH was adjusted to 4.5 using NaOH and phages were added to a final concentration of $\sim 10^9$ plaque forming units/ml (PFU/ml). Two aqueous solutions of 5% wt/v TPP and 5% v/v GPTMS were added together 1 ml each, drop wise, into 10 ml of the continuously stirred chitosan-phage solution, completing the encapsulation process. The resulting suspension was centrifuged at 10,000 g for 10 min to collect the encapsulated phages, which were washed three times with pH 7 tap water and stored in 10 ml of pH 7 tap water at room temperature and shaken vigorously before use. Empty encapsulation suspension was made following the same steps but without addition of phages to control for the effect of the encapsulation itself.

Synthesis of encapsulated phages is limited by concentration of encapsulating nanomaterials (i.e., chitosan, TPP, and GTPMS). However, when the chitosan concentration is about 10 mg/ml (twice the concentration used in this study), the solution becomes too viscous and difficult to work with since it cannot be stirred magnetically with a stir bar. Thus, viscosity of the chitosan solution limits the concentration of phages that can be encapsulated. Furthermore, while the encapsulated phages are protected from the acidic pH of the chitosan solution (pH 4.5), the unencapsulated free phages are continuously degraded by this acidic pH. Therefore, the concentration of phages added during production ($\sim 10^9$ PFU/ml) is oversaturated to ensure maximum encapsulation; however, this results in around just ~1% of phages used in production that can be released as viable phages ($\sim 10^7$ PFU/ml) from the encapsulation. Further optimization is still required to improve this low percentage, though compared to encapsulating more expensive therapeutic drugs, this is less consequential since the exponential self-propagation of phages makes phage production fast and relatively inexpensive (Anam et al., 2020; Luong et al., 2020).

2.3. Coating plasma-treated surfaces with encapsulated phages

High-density polyethylene (HDPE) from NALGENE was cut into discs 35 and 16 mm in diameter that could be fitted into individual wells of 6 and 24 well plates respectively. The HDPE discs were wiped with ethanol to clean the surfaces as a pretreatment measure. Plasma treatment was then performed for 5 min using Fischione model 1020 plasma cleaner with 25% oxygen + 75% argon gas mix. The plasma-treated HDPE discs were dip coated into 1 ml suspension of either encapsulated phages or empty encapsulation, which instantly formed a coating.

2.4. Biofilm biomass measurements

The smaller 16-mm HDPE discs fitted for 24-well plates used for other experiments in this study did not form enough total biofilm biomass to facilitate quantification. Thus, larger 35-mm HDPE discs were used. These disks were coated with encapsulated phages or with empty encapsulations or left uncoated as controls and were taped to the

bottom of each well in a 6-well plate. Then, tap water (5 ml, unfiltered and used as is) amended with 200 mg/L glucose and 250 μl of a *P. aeruginosa* PAO1 overnight culture (~0.4 OD_{600nm}) was added to each well, and samples were collected after 3 days at 30°C to quantify total biofilm biomass. The concentration of *P. aeruginosa* and glucose used for biofilm experiments is relatively high for water systems, but allowed us to work with sufficient biomass to more easily quantify the effect of phages and limit potential interactions between phages and non-target bacterial species.

A modified crystal violet (CV) assay was used for biomass quantification. CV is often used for colorimetric quantification of biofilm biomass (Azeredo et al., 2017), but it binds to the chitosan coating as well as to the biofilm, confounding results. Thus, biofilms were first resuspended to separate them from the chitosan coating. This procedure was used for all treatments and the biofilm biomass measurements are presented as percentages relative to the uncoated control. Briefly, biofilms were resuspended into 1 ml PBS by sonication at 40 kHz for 5min in a bath sonicator (Branson, Danbury, CT), mixed by pipetting up and down 10 times, and transferred into a 1.5 ml centrifuge tube. Then, 50 μl of the resuspended biofilm in PBS was set aside for enumeration using viable plate counts. Next, 50 μl of a 1% wt/vol CV aqueous solution was added to reach a concentration of 0.05% wt/vol CV in the tubes. After 15 min incubation in the dark at room temperature, the tube was centrifuged at 13,000 g for 5 min to pellet the resuspended biofilm. The pellet was washed 5 times with PBS to remove residual CV in the supernatant. Then, 1 ml of 70% ethanol was added, and the tube was incubated again for 15 min and inverted 10 times to release the CV in the biofilm pellet. Finally, 200 μl from each tube was transferred into a clean 96-well plate and absorbance at 595 nm was measured using a Tecan Infinite 200 Pro plate reader.

2.5. Live/dead cells staining

To assess biofilms via live/dead staining, biofilms were grown on 16-mm HDPE discs coated with empty encapsulation or encapsulated phages or uncoated controls. These discs were taped into individual wells of a 24-well plate and submerged in 2 ml tap water (pH 7.6) amended with 200 mg/L glucose and inoculated with 100 μl of a *P. aeruginosa* overnight culture (~0.4 OD_{600nm}). After 3 days at 30°C, media and planktonic cells were pipetted out of each well and the remaining biofilm was washed by gently adding and removing 1 ml PBS to remove any remaining planktonic cells. The staining solution (200 μl of 7.5 μM SYTO 9 and 30 μM propidium iodide in DI) was added to each well and the plate was incubated in the dark for 15 min. To avoid the HDPE discs from interfering with measurements, the biofilm was resuspended into the staining solution which was then transferred to a clean 96-well black-walled plate. Using Tecan Infinite 200 Pro plate reader with excitation wavelength at 485 nm, fluorescence intensities at 535 nm (SYTO 9 green emission for live cells) and 635 nm (propidium iodide red emission for dead cells) were measured. The ratio of live to dead cells within each individual biofilm on uncoated and coated surfaces was obtained by dividing the fluorescence intensity corresponding to green, live cells by that of the red, dead cells.

2.6. Biofilm visualization and pH measurement using confocal laser scanning microscopy

Biofilms were formed on 16-mm HDPE discs after 3 days at 30°C as described above. The biofilms were then fixed onto the HDPE discs using methanol and carbon tape was used to attach the discs onto a glass slide. Next, 100 μl of the live/dead staining solution was added to the biofilm and incubated in the dark for 30 min, and one drop of ProLong gold antifade (Thermo Fisher) was added to the biofilm and covered with a No. 1.5 cover slip. The sample was observed using a 20X dry objective using Nikon A1-Rsi confocal laser scanning microscope (CLSM). Z-stack image were collected, and 3D images of the biofilm was generated using Nikon NIS-Element software. Images were acquired with excitation wavelength of 488 nm and emission wavelength from 500 to 550 nm for viable live bacteria stained with SYTO 9, and excitation wavelength of 560 nm with emission wavelength from 570 to 620 nm for non-viable dead bacteria stained with propidium iodide. Images were 512 by 512 pixels in size and pixel dwell time was 2.4 μs with 2X line averaging.

For pH measurements, biofilms were formed as described above, but not fixed with methanol, and were stained with 100 μl of 20 μM SNARF-4F in tap water amended with 200 mg/L glucose instead. Calibration for pH was generated using 20 μM SNARF-4F in pH-adjusted tap water ranging from pH 5 to 8 (Fig. S1). CLSM images were acquired using 40X dry objective with 4X line averaging for higher resolution, which is more relevant for discerning acidic microenvironments than image size. The excitation wavelength was 488 nm and emission wavelengths were measured from 550 to 610 nm (green) and 610 to 670 nm (red). No autofluorescence was detected in unstained biofilms. ImageJ software with Ratio Plus plugin (https://imagej.nih.gov/ij/plugins/ratio-plus.html) was used to generate images based on green/red fluorescence ratio (Fulaz et al., 2019). To approximate the trend of pH distributions within biofilms, images were background-subtracted and clipped to reduce noise, mean and median filtered, and false colored with a look up table modified based on pH scale calibrations (Fig. S1).

2.7. Measuring release of encapsulated phages

The number of phage particles was determined through double-layer plaque assay. To test the effect of pH on phage release, 10 μl of encapsulated phage suspension was added to 1 ml tap water or adjusted to various pH (7, 6, and 5) using HCl and incubated for 1 h at room temperature. To test effect of salt concentration on phage release, the same steps were taken but using 1 ml solutions of NaCl (0.1 and 0.01 M) and $CaCl_2$ (0.01 and 0.001 M) in tap water with an unadjusted pH of 7.6 instead. Afterwards, the incubated phages were added along with 50 μl of a *P. aeruginosa* PAO1 overnight culture to 5 ml of ~50°C TSB agar, poured onto the base layer, inverted after solidifying, and incubated overnight at 30°C. The experiment was repeated after encapsulated phages were stored for 1 month in pH 7 tap water at room temperature to determine longer term stability.

2.8. Scanning electron microscopy (SEM) imaging and nanoparticle size measurement

Encapsulated phage suspension (10 μl) was pipetted onto carbon tape on SEM pin stubs from Electron Microscopy Sciences and air dried. Samples were then sputter coated with 10 nm layer of gold using Denton Vacuum DESK V. Samples were then visualized with a FEI Helios Nanolab 660 SEM/FIB operated at an accelerating voltage of 20 kV. ImageJ software was used to measure 100 nanoparticles to determine average size and standard deviation.

2.9. Measuring phage release from surface coating

Flat HDPE and fiberglass squares (1 cm^2) where plasma treated and coated with encapsulated phages as described in Section 2.3. The HDPE and fiberglass squares were then incubated in 5 ml pH 7.6 and pH 5 tap water for 1 h at 30°C without shaking. The number of phage particles released from the coating into the tap water was then determined by the double-layer plaque assay.

2.10. Statistical analysis

Experiments were run as independent triplicates. Student's t-test (two-tailed, unpaired, assuming equal variance) was used to determine if differences in phage plaque forming units, bacterial optical density, and fluorescence intensity were significant at the 95% confidence level (i.e., $p < 0.05$).

3. Results & discussion

3.1. *Pseudomonas aeruginosa PAO1 triggered and was subsequently controlled by release of encapsulated phages, mitigating biofilm formation*

Crystal violet staining showed that relative biofilm biomass was significantly lower for biofilms formed on HDPE plastic coated with encapsulated phages (6.7 ± 0.2%) than for the empty encapsulation coating (95.3 ± 3.2%) and uncoated controls (100 ± 10.5%, Fig. 1A). This was corroborated by viable count assays showing that encapsulated phage coating resulted in a much lower biofilm surface area coverage (4.8 ± 0.2 log CFU/mm^2) compared to the empty encapsulation coating (6.8 ± 0.3 log CFU/mm^2) and uncoated controls (6.6 ± 0.2 log CFU/mm^2, Fig. 1A).

Live/dead viability assay was performed on the biofilms using SYTO 9 to stain viable live cells and propidium iodide to stain non-viable dead cells. For biofilms formed on HDPE plastic surfaces coated with encapsulated phages, fluorescence intensity in arbitrary units (a.u.) corresponding to viable live cells (4,578 ± 362 a.u.) was lower than biofilms formed on empty encapsulation coating (23,545 ± 1,716 a.u.) and the uncoated controls (23,170 ± 1,579 a.u., Fig. 1B). Conversely, fluorescence intensity corresponding to non-viable dead cells were 2,537 ± 50, 2,137 ± 64, and 2,097 ± 140 a.u. respectively for biofilms grown on HDPE plastic with encapsulated phages coating, empty encapsulation coating, and uncoated controls (Fig. 1B). Thus, biofilms formed on HDPE plastic with encapsulated phage coating had fluorescence intensities that were much lower for viable live cells and slightly higher for non-viable dead cells, resulting in a live/dead fluorescence ratio of 1.80; this was lower than both the empty encapsulation coating (live/dead ratio of 11.02), and uncoated controls (live/dead ratio of 11.05, Fig. 1B).

Mitigation of biofilms by encapsulated phage coating was visualized and confirmed by CLSM, which showed that biofilm formation on uncoated control and empty encapsulation coating was much greater than on HDPE surfaces with encapsulated phage coating (Fig. 1C). Here, phage release from encapsulation was autonomously triggered by the biofilm formed in tap water with a slightly basic bulk volume pH of 7.6, enabling phages to be released only as needed. Note that dissolved biocides do not target biofilm locations with precision, possibly wasting some treatment capacity on side reactions over the entire bulk volume (Armbruster et al., 2015). This coating process allows precise mitigation for the bottom surface of storage tanks, where bacteria typically settle and attach. Phages are released from under the biofilm and target the inner layer of biofilms, using a bottom-up approach that avoids the challenge of limited penetration through the outer biofilm matrix. The encapsulated phages would target the early stages of biofilm formation from the bottom surface (i.e., a bottom-up approach). Previous studies have shown enhanced efficacy of the bottom-up approach to biofilm control compared to free phages, which have limited penetration through the biofilm matrix and are diluted throughout the bulk volume instead of concentrated on the biofilm interface (Yu et al., 2019). Additionally, targeting early colonizers like *Pseudomonas* spp. may also hinder or even prevent subsequent attachment by other species that do not initiate surface attachment (Douterelo et al., 2014; Liu et al., 2016).

In this study, experiments were run for 3 days to obtain proof-of-concept of biofilm mitigation. However, further studies at larger temporal and spatial scales are needed to establish the feasibility of this promising approach. A potential limitation would be bacteria developing resistant to phage infections. This could be addressed, in part, by encapsulating a cocktail of broad-host range phages, or by rotating phages when the coating is replenished (Lewis and Hill, 2020). Furthermore, bacterial resistance to phages come with a fitness cost that slows host growth and increases susceptibility to disinfectants

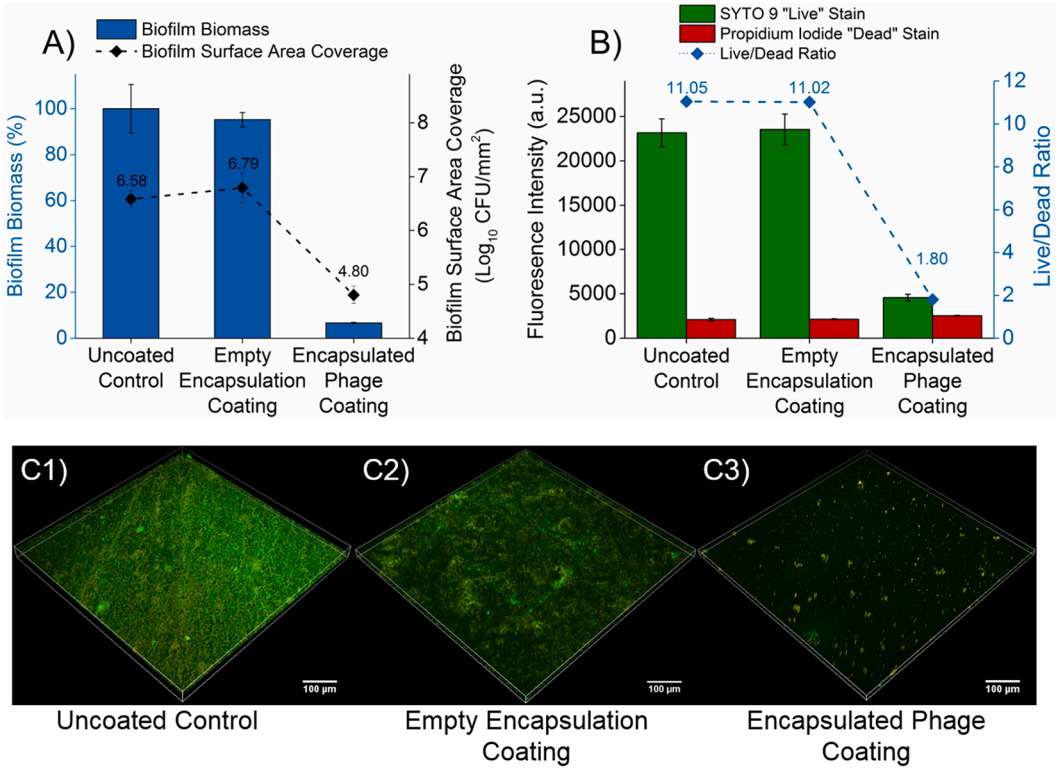

Fig. 1. (A) Encapsulated phage coating significantly suppressed *P. aeruginosa* PAO1 biofilm formation on high-density polyethylene (HDPE) plastic after 3 days at 30°C in tap water (pH 7.6) amended with 200 mg/L glucose, as shown by the lower biofilm biomass and surface area coverage compared to the control. **(B)** Biofilm live/dead staining show lower live/dead ratio and fluorescence intensity corresponding to live biofilm bacteria on HDPE surfaces coated with encapsulated phages. **(C)** CLSM imaging of biofilm formation on uncoated and coated HDPE surfaces. Biofilms were stained with SYTO 9 and propidium iodide such that live and dead cells respectively appear green and red. Error bars represent ± one standard deviation from the mean of independent triplicates.

(Mangalea and Duerkop, 2020; Yu et al., 2017). Another potential limitation is low temperatures, since very few phages can infect and lyse bacteria at temperatures lower than 7°C (Jurczak-Kurek et al., 2016). However, biofouling would also be mitigated by low temperatures.

3.2. Encapsulated phages are stable for over 1 month in pH neutral tap water, and phage release can be triggered by low pH

Release of encapsulated phages can be triggered by low pH. This was demonstrated by incubating encapsulated phages for 1 h in room-temperature tap water adjusted to various pH values (5, 6, and 7) using HCl. After 1 h of incubation in pH 5 and pH 6 tap water, 7.60 ± 0.03 and 4.65 ± 0.01 log PFU/ml of phages were respectively released from the stock suspension of encapsulated phages, but in pH 7 tap water, the normal storage condition, there was only 2.94 ± 0.25 log PFU/ml of released phages (Fig. 2A). This is attributed to unencapsulated phages that were not removed by the washing step and represents a negligible amount in the context of source depletion when phage release is not needed. This experiment was repeated after encapsulated phages were left in pH 7 tap water at room temperature for 1 month to assess longer term viability. After one-month, encapsulated phages incubated for 1 h in pH 7, 6, and 5 tap water resulted in release of 3.29 ± 0.10, 4.19 ± 0.21, and 7.22 ± 0.08 log PFU/ml of phages (Fig. 2A). This pattern suggests a slight leakage of phages from the encapsulation over time, but the differences are minor and negligible on a log scale. Thus, in the absence of bacteria, the vast majority of the encapsulated phages would not be wastefully released or decay for at least 1 month when phage release is not needed.

Chitosan crosslinked with GPTMS is known to be pH responsive. At low pH, proton solvation imparts positive charge to various functional groups (e.g., carboxylate and amino groups), leading to electrostatic repulsion between the now positively charged groups which causes swelling of the encapsulation and subsequent release of its cargo (Li et al., 2020). This pH sensitivity is dependent on the GPTMS mass ratio (i.e., higher ratios of GPTMS will increase pH sensitivity and vice versa) (Wu and Sailor, 2009). Thus, this allows the pH responsiveness of the encapsulation to be adjusted and optimized for delivery and cargo release in different environments.

Ratiometric pH indicator dye, SNARF-4F, was used to measure pH ranges within *P. aeruginosa* biofilms to determine whether phage release could be autonomously triggered. Biofilm pH colormaps were generated from CLSM images, and showed that acidic microenvironments were scattered throughout the biofilm, with pH as low as 5.3 (especially in the inner layers close to the biofouled surface), which is acidic enough to trigger phage release and autonomously exert biofouling control (Fig. 2B). This result is supported by previous research which used the same pH indicator dye and reported pH as low as 5.6 (which was their limit of detection) within *P. aeruginosa* biofilms (Hunter and Beveridge, 2005). Additionally, pH as low as 5.1 has also been found in *Pseudomonas fluorescens* biofilm inner layers (Fulaz et al., 2019). Apparently, limited oxygen penetration into biofilm inner layers create anoxic microenvironments leading to glycolysis and acidic fermentation by-product (e.g., lactic and acetic acid) build up, which in turn, creates an acidic microenvironment (Hu et al., 2019). These processes are not species specific, so most biofilm inner layers have acidic pH and can be broadly targeted by pH responsive antimicrobial delivery systems (Chen et al., 2018).

Incidentally, previous biomedical studies have similarly exploited pH gradients to enhance selective treatment. For example, healthy tissues (have slightly basic pH 7.4) were avoided in efforts to selectively target methicillin-resistant *Staphylococcus aureus* biofilm infections (pH 5.5) in rabbits by heat-killing gold nanoparticles (Peng et al., 2021). A similar approach also worked for targeting *S. aureus* biofilm infections (pH 5.0) rather than healthy tissues in mice (pH 7.4) (Zhao et al., 2019). Additionally, pH responsive nanoparticles have been used to deliver antimicrobial agents to oral biofilms (pH 5 ~ 5.5) and avoid nonspecific release into healthy oral tissues (pH 7.4) (Niaz et al., 2020; Zhao et al., 2019). Tap water generally has a slightly basic pH similar to the pH of healthy tissues avoided by pH-responsive nanoparticles (Salehi et al., 2020; Zhang et al., 2015). Thus, by using an encapsulation with similar pH responsiveness (i.e., stable at neutral/slightly basic pH and release at acidic pH), we could protect the encapsulated phages from unintended release into sterile tap water and selectively target nascent biofilms.

3.3. Phage release could be inadvertently triggered by high salt concentrations, but not by low salinity found in drinking water systems

The ability of hydrogen ions (at low pH) to trigger phage release raises the concern that sodium and calcium cations, which are common in tap water, could unintentionally do the same. Thus, we also examined how fluctuations in water chemistry can affect encapsulation stability. Phage release from encapsulations could be triggered by 5,840 mg/L or 0.1 M NaCl (7.03 ± 0.20 log PFU/ml) and 1,110 mg/L or 0.01 M $CaCl_2$ (7.21 ± 0.09 log PFU/ml, Fig. 3). However, when lower concentrations were used (i.e., 584 and 111 mg/L or 0.01 or 0.001 M of NaCl and $CaCl_2$, respectively), the concentration of phages detected was only 3.51 ± 0.09 and 2.96 ± 0.20 log PFU/ml, respectively, which is comparable to the number of phages passively released in unadjusted pH 7.6 tap water. Thus, while phage release is less sensitive to sodium and calcium ions than to low pH, high concentrations of sodium and calcium chloride (i.

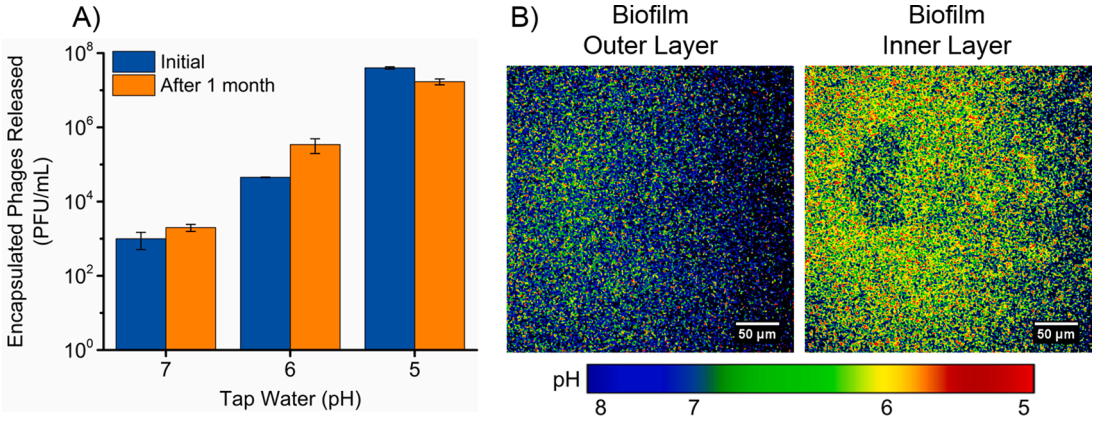

Fig. 2. **(A)** Encapsulated phages are stable for at least one month in tap water (pH 7) and phage release is gradually triggered as pH decreases to 5. **(B)** Biofilm inner layers show heterogenous pH distribution with domains where pH could be as low as 5.3, which could trigger phage release. To show a general overview of pH patterns within biofilms, ratiometric images were generated and processed using ImageJ software based on CLSM imaging of *P. aeruginosa* biofilm stained with ratiometric pH indicator SNARF-4F. Error bars represent ± one standard deviation from the mean of independent triplicates.

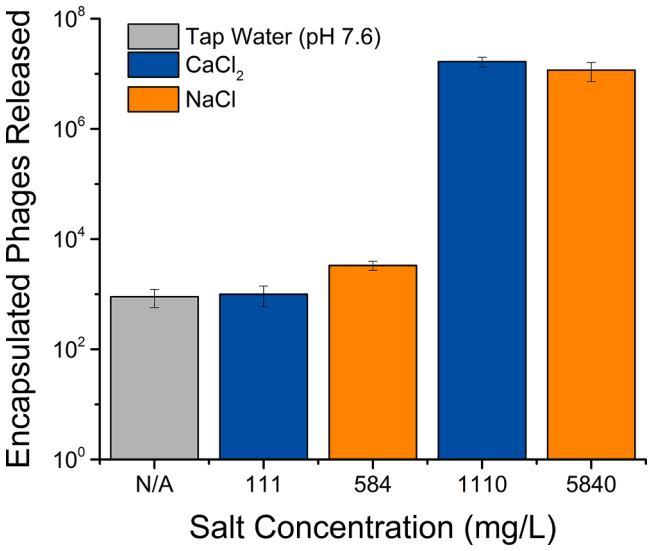

Fig. 3. Phage release from encapsulation can also be triggered by 5,840 mg/L (or 0.1 M) of NaCl or 1,110 mg/L (0.01 M) of $CaCl_2$ in tap water (pH 7.6), but not by lower salt concentrations typically found in drinking water. Error bars represent ± one standard deviation from the mean of independent triplicates.

e., 5,840 and 1,110 mg/L or 0.1 and 0.01 M, respectively) can still trigger phage release comparable to pH 5 (or 0.00001 M H^+) at around 7 log PFU/ml (Fig. 3). However, there is little concern with unintended phage release triggered by fluctuations in water chemistry and salinity because the ion concentrations required are above secondary drinking water standards of 500 mg/L for total dissolved solids and 250 mg/L for chloride (USEPA, 1979). Thus, under most tap water conditions, the encapsulated phages should remain stable.

We ruled out the possibility of phage release due to biodegradation of the encapsulating materials, which is unlikely to provide nutrients and promote biofouling. Specifically, we examined growth of *P. aeruginosa* PAO1 after one-week incubation at 30°C in tap water (unadjusted pH of 7.6) amended with 3.6 or 0.36 g/L of either glucose or empty chitosan encapsulations. When the carbon source was 3.6 or 0.36 g/L glucose, *P. aeruginosa* PAO1 reached an optical density of 0.54 ± 0.02 and 0.17 ± 0.01 OD_{600nm}, respectively (Fig. S2). However, when glucose was replaced with empty chitosan encapsulations instead, optical density after 1 week was only 0.008 ± 0.013 and 0.004 ± 0.0004 OD_{600nm}, respectively, indicating that no growth occurred (Fig. S2). Chitosan is known to be biodegradable, but degradation rates are lower for chitosan with higher degrees of deacetylation (85% deacetylated chitosan used in this study), which can take multiple months to biodegrade (Kurita, 2006; Ren et al., 2005). Since 5 ml of tap water was inoculated with 100 µl of *P. aeruginosa* PAO1, bacterial presence is much higher than normal conditions for this experiment, but still no growth was detected. While biodegradation may still be possible on a longer time scale, the coating method greatly lowers chitosan concentration used for biofilm mitigation and that could be inadvertently biodegraded.

3.4. Encapsulated phages adhere to plasma-treated plastic and fiberglass surfaces upon contact, enabling an instant method of coating biofouling-susceptible surfaces

The chitosan encapsulation enabled this simple coating method which resulted in a visibly rougher texture after dip coating of plasma treated materials into the encapsulated phage suspension (Fig. 4A). To determine whether efficacy of the encapsulated phage coating process is affected by different surface materials, phage release patterns from HDPE and fiberglass, both common materials used to make water storage tanks, were examined. Plasma treated HDPE and fiberglass surfaces with encapsulated phage coating were able to release 3.75 ± 0.05 and 3.58 ± 0.12 log PFU/cm^2 of phages, respectively, when exposed to pH 5 tap water compared to the 1.40 ± 0.14 and 1.55 ± 0.43 log PFU/cm^2 of phages released in normal pH 7.6 tap water (Fig. 4B). Thus, low pH can trigger comparable phage release from coatings on both surface materials., demonstrating that the coating process is equally effective for two of the most common materials used for water storage tanks.

Previous studies have attributed this coating process to the formation hydrogen bonds between hydroxyl groups on the plasma treated plastic surface and hydroxyl or amino groups on the chitosan (Suganya et al., 2018). Since this hydrogen bonding occurs on the carbon chain and does not involve functional groups specific to different kinds of plastic, the coating process is versatile and applicable to other plastics such as polyvinylchloride (PVC) and polystyrene as well. Additionally, there are various other methods such as corona treatment that could replace

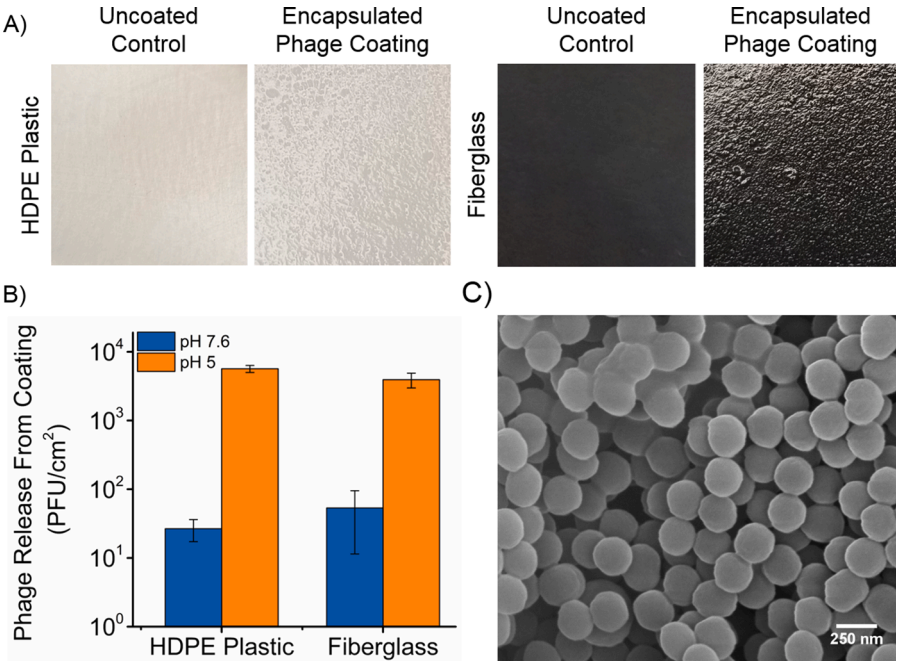

Fig. 4. (A) Dip coating plasma treated HDPE plastic and fiberglass surfaces into encapsulated phage suspension results in a visibly rougher surface texture. **(B)** Encapsulated phage coating on both HDPE plastic and fiberglass surfaces have comparable phage release profiles in tap water (pH 7.6 and 5), inferring that phage release from coating is independent of the surface material. **(C)** SEM imaging show that crosslinked chitosan form spheres with an average diameter of 244 ± 11 nm based on size measurement of 100 particles using ImageJ software. Error bars represent ± one standard deviation from the mean of independent triplicates.

plasma treatment to increase the free surface energy and facilitate coating of encapsulated phages (Munteanu et al., 2014).

In addition to facilitating this coating process, the chitosan encapsulation has other advantageous properties worth noting. Most phages range from 20 to 200 nm (Sulcius et al., 2011) in size and the phage used in this study is 86 nm (Yu et al., 2019). In comparison, the crosslinked chitosan with TPP and GTMPS formed uniformly sized spheres 244 ± 11 nm in diameter (Fig. 4C). This is much smaller than previously reported alginate-based phage encapsulations (including alginate-chitosan encapsulations) which usually had diameters in the micrometer range (Abdelsattar et al., 2019; Colom et al., 2017; Soto et al., 2018). The smaller encapsulation size here is more in line with other chitosan-based encapsulations and is conducive to higher surface area to volume ratios, and thus, more direct contact between the encapsulated phages and their bacterial targets (Xu et al., 2019). Additionally, we previously found that smaller phage-nanoparticle-conjugates disperse phages more evenly than their larger counterparts, and therefore, cause greater disruption of biofilm inner layers and are more efficient at biofilm removal (Yu et al., 2019). Finally, chitosan, TPP, and select phage products are all generally regarded as safe (i.e., GRAS status) by the U.S. Food and Drug Administration, while GPTMS is an indirect additive used in food contact substances (Garg et al., 2019; Silano et al., 2017; Wu et al., 2017). Thus, unlike DBPs that can be carcinogenic, the phages encapsulated in chitosan, TPP, and GPTMS raise no concerns with regards to public health.

4. Conclusion

The use of chemical disinfectants for biofilm eradication faces several drawbacks, including low efficacy due to limited biofilm penetration and the generation of harmful DBPs. Phages are self-propagating green biocides that can provide a chemical-free alternative to biofilm control. Encapsulating phages in crosslinked chitosan enabled autonomous release of the bactericidal phage cargo in response to biofilm formation, but otherwise remains stable in room temperature tap water for at least one month. The encapsulated phages could also be selectively coated onto surfaces to precisely mitigate biofouling where it is needed. This method allows for increased precision for targeting where nascent biofilms form using a bottom-ups approach that bypasses the problem of limited penetration through the biofilm matrix. Overall, we present a simple technology for small-scale point of use applications and to complement established water treatment methods to curtail chemical intensity for improving water safety.

Declaration of Competing Interest

We declare that we have no known competing financial interests or personal relationships that could have appeared to influence the work reported in this paper.

Data availability

No data was used for the research described in the article.

Acknowledgements

Funding for this project was provided by the National Science Foundation through the Engineering Research Center (ERC) for Nanotechnology-Enabled Water Treatment (NEWT) (EEC-1449500).

Supplementary materials

Supplementary material associated with this article can be found, in the online version, at doi:10.1016/j.watres.2022.119070.

References

Abdelsattar, A.S., Abdelrahman, F., Dawoud, A., Connerton, I.F., El-Shibiny, A., 2019. Encapsulation of E. coli phage ZCEC5 in chitosan–alginate beads as a delivery system in phage therapy. AMB Express 9, 1–9.
Anam, G.B., Yadav, S., Ayyaru, S., Ahn, Y.-H., 2020. Nanocomposite membrane integrated phage enrichment process for the enhancement of high rate phage infection and productivity. Biochem. Eng. J. 163, 107740.
Armbruster, D., Happel, O., Scheurer, M., Harms, K., Schmidt, T.C., Brauch, H.-J., 2015. Emerging nitrogenous disinfection byproducts: transformation of the antidiabetic drug metformin during chlorine disinfection of water. Water Res. 79, 104–118.
Azeredo, J., Azevedo, N.F., Briandet, R., Cerca, N., Coenye, T., Costa, A.R., Desvaux, M., Di Bonaventura, G., Hébraud, M., Jaglic, Z., 2017. Critical review on biofilm methods. Crit. Rev. Microbiol. 43, 313–351.
Bridier, A., Briandet, R., Thomas, V., Dubois-Brissonnet, F., 2011. Resistance of bacterial biofilms to disinfectants: a review. Biofouling 27, 1017–1032.
Centurion, F., Basit, A.W., Liu, J., Gaisford, S., Rahim, M.A., Kalantar-Zadeh, K., 2021. Nanoencapsulation for probiotic delivery. ACS Nano 15, 18653–18660. https://doi.org/10.1021/acsnano.1c09951.
Chao, Y., Mao, Y., Wang, Z., Zhang, T., 2015. Diversity and functions of bacterial community in drinking water biofilms revealed by high-throughput sequencing. Sci. Rep. 5, 1–13.
Chen, H., Jin, Y., Wang, J., Wang, Y., Jiang, W., Dai, H., Pang, S., Lei, L., Ji, J., Wang, B., 2018. Design of smart targeted and responsive drug delivery systems with enhanced antibacterial properties. Nanoscale 10, 20946–20962.
Colom, J., Cano-Sarabia, M., Otero, J., Aríñez-Soriano, J., Cortés, P., Maspoch, D., Llagostera, M., 2017. Microencapsulation with alginate/$CaCO_3$: a strategy for improved phage therapy. Sci. Rep. 7, 1–10.
de Jonge, P.A., Nobrega, F.L., Brouns, S.J.J., Dutilh, B.E., 2019. Molecular and evolutionary determinants of bacteriophage host range. Trends Microbiol. 27, 51–63.
Douterelo, I., Sharpe, R., Boxall, J., 2014. Bacterial community dynamics during the early stages of biofilm formation in a chlorinated experimental drinking water distribution system: implications for drinking water discolouration. J. Appl. Microbiol. 117, 286–301.
Du, H., Liu, M., Yang, X., Zhai, G., 2015. The design of pH-sensitive chitosan-based formulations for gastrointestinal delivery. Drug Discov. Today 20, 1004–1011.
Flemming, H.-C., Wingender, J., Szewzyk, U., Steinberg, P., Rice, S.A., Kjelleberg, S., 2016. Biofilms: an emergent form of bacterial life. Nat. Rev. Microbiol. 14, 563–575.
Flemming, H.-C., Wuertz, S., 2019. Bacteria and archaea on Earth and their abundance in biofilms. Nat. Rev. Microbiol. 17, 247–260.
Fulaz, S., Hiebner, D., Barros, C.H.N., Devlin, H., Vitale, S., Quinn, L., Casey, E., 2019. Ratiometric imaging of the *in situ* pH distribution of biofilms by use of fluorescent mesoporous silica nanosensors. ACS Appl. Mater. Interfaces 11, 32679–32688.
Garg, U., Chauhan, S., Nagaich, U., Jain, N., 2019. Current advances in chitosan nanoparticles based drug delivery and targeting. Adv. Pharm. Bull. 9, 195.
Haller, L., Chen, H., Ng, C., Le, T.H., Koh, T.H., Barkham, T., Sobsey, M., Gin, K.Y.-H., 2018. Occurrence and characteristics of extended-spectrum β-lactamase-and carbapenemase-producing bacteria from hospital effluents in Singapore. Sci. Total Environ. 615, 1119–1125.
Herrera, G., Peña-Bahamonde, J., Paudel, S., Rodrigues, D.F., 2021. The role of nanomaterials and antibiotics in microbial resistance and environmental impact: an overview. Curr. Opin. Chem. Eng. 33, 100707.
Hicks, E., Wiesner, M.R., Gunsch, C.K., 2020. Modeling bacteriophage-induced inactivation of Escherichia coli utilizing particle aggregation kinetics. Water Res. 171, 115438.
Hu, D., Deng, Y., Jia, F., Jin, Q., Ji, J., 2019. Surface charge switchable supramolecular nanocarriers for nitric oxide synergistic photodynamic eradication of biofilms. ACS Nano 14, 347–359.
Hunter, R.C., Beveridge, T.J., 2005. Application of a pH-sensitive fluoroprobe (C-SNARF-4) for pH microenvironment analysis in Pseudomonas aeruginosa biofilms. Appl. Environ. Microbiol. 71, 2501–2510.
Jurczak-Kurek, A., Gąsior, T., Nejman-Faleńczyk, B., Bloch, S., Dydecka, A., Topka, G., Necel, A., Jakubowska-Deredas, M., Narajczyk, M., Richert, M., 2016. Biodiversity of bacteriophages: morphological and biological properties of a large group of phages isolated from urban sewage. Sci. Rep. 6, 1–17.
Kurita, K., 2006. Chitin and chitosan: functional biopolymers from marine crustaceans. Mar. Biotechnol. 8, 203–226.
Lewis, R., Hill, C., 2020. Overcoming barriers to phage application in food and feed. Curr. Opin. Biotechnol. 61, 38–44.
Li, C.-P., Weng, M.-C., Huang, S.-L., 2020. Preparation and characterization of pH sensitive chitosan/3-glycidyloxypropyl trimethoxysilane (GPTMS) hydrogels by sol-gel method. Polymers (Basel) 12, 1326.
Liu, L., Yao, W., Rao, Y., Lu, X., Gao, J., 2017. pH-Responsive carriers for oral drug delivery: challenges and opportunities of current platforms. Drug Deliv. 24, 569–581.
Liu, S., Gunawan, C., Barraud, N., Rice, S.A., Harry, E.J., Amal, R., 2016. Understanding, monitoring, and controlling biofilm growth in drinking water distribution systems. Environ. Sci. Technol. 50, 8954–8976.
Luong, T., Salabarria, A.-C., Edwards, R.A., Roach, D.R., 2020. Standardized bacteriophage purification for personalized phage therapy. Nat. Protoc. 15, 2867–2890.
Mangalea, M.R., Duerkop, B.A., 2020. Fitness trade-offs resulting from bacteriophage resistance potentiate synergistic antibacterial strategies. Infect. Immun.
Mortimer, M., Devarajan, N., Li, D., Holden, P.A., 2018. Multiwall carbon nanotubes induce more pronounced transcriptomic responses in Pseudomonas aeruginosa

PG201 than graphene, exfoliated boron nitride, or carbon black. ACS Nano 12, 2728–2740.
Munteanu, B.S., Paslaru, E., Zemljic, L.F., Sdrobis, A., Pricope, G.M., Vasile, C., 2014. Chitosan coatings applied to polyethylene surface to obtain food-packaging materials. Cell. Chem. Technol. 48, 565–575.
Niaz, T., Shabbir, S., Noor, T., Abbasi, R., Imran, M., 2020. Alginate-caseinate based pH-responsive nano-coacervates to combat resistant bacterial biofilms in oral cavity. Int. J. Biol. Macromol. 156, 1366–1380.
Peng, D., Liu, G., He, Y., Gao, P., Gou, S., Wu, J., Yu, J., Liu, P., Cai, K., 2021. Fabrication of a pH-responsive core–shell nanosystem with a low-temperature photothermal therapy effect for treating bacterial biofilm infection. Biomater. Sci. 9, 7483–7491.
Ren, D., Yi, H., Wang, W., Ma, X., 2005. The enzymatic degradation and swelling properties of chitosan matrices with different degrees of N-acetylation. Carbohydr. Res. 340, 2403–2410.
Salehi, M., Odimayomi, T., Ra, K., Ley, C., Julien, R., Nejadhashemi, A.P., Hernandez-Suarez, J.S., Mitchell, J., Shah, A.D., Whelton, A., 2020. An investigation of spatial and temporal drinking water quality variation in green residential plumbing. Build. Environ. 169, 106566.
Schlafer, S., Garcia, J.E., Greve, M., Raarup, M.K., Nyvad, B., Dige, I., 2015. Ratiometric imaging of extracellular pH in bacterial biofilms with C-SNARF-4. Appl. Environ. Microbiol. 81, 1267–1273.
Silano, V., Bolognesi, C., Chipman, K., Cravedi, J.P., Engel, K., Fowler, P., Grob, K., Gürtler, R., Husøy, T., Kärenlampi, S., 2017. Safety assessment of the substance [3-(2, 3-epoxypropoxy) propyl] trimethoxy silane, for use in food contact materials.
Soto, M.J., Retamales, J., Palza, H., Bastías, R., 2018. Encapsulation of specific Salmonella Enteritidis phage f3αSE on alginate-spheres as a method for protection and dosification. Electron. J. Biotechnol. 31, 57–60. https://doi.org/10.1016/j.ejbt.2017.11.006.
Stachler, E., Kull, A., Julian, T.R., 2021. Bacteriophage treatment before chemical disinfection can enhance removal of plastic-surface-associated pseudomonas aeruginosa. Appl. Environ. Microbiol. 87, e00921–e00980.
Suganya, A., Shanmugvelayutham, G., Hidalgo-Carrillo, J., 2018. Plasma surface modified polystyrene and grafted with chitosan coating for improving the shelf lifetime of postharvest grapes. Plasma Chem. Plasma Process. 38, 1151–1168.
Sulcius, S., Staniulis, J., Paškauskas, R., 2011. Morphology and distribution of phage-like particles in a eutrophic boreal lagoon. Oceanologia 53, 587–603.
Tanner, W.D., VanDerslice, J.A., Goel, R.K., Leecaster, M.K., Fisher, M.A., Olstadt, J., Gurley, C.M., Morris, A.G., Seely, K.A., Chapman, L., 2019. Multi-state study of Enterobacteriaceae harboring extended-spectrum beta-lactamase and carbapenemase genes in US drinking water. Sci. Rep. 9, 1–8.
USEPA, 1979. National Secondary Drinking Water Regulations EPA 570/9-76-000. Washington DC.
Wu, J., Sailor, M.J., 2009. Chitosan hydrogel-capped porous SiO_2 as a pH responsive nano-valve for triggered release of insulin. Adv. Funct. Mater. 19, 733–741.
Wu, J., Wang, Y., Yang, H., Liu, X., Lu, Z., 2017. Preparation and biological activity studies of resveratrol loaded ionically cross-linked chitosan-TPP nanoparticles. Carbohydr. Polym. 175, 170–177.
Xu, J., Liu, Y., Li, Y., Wang, H., Stewart, S., Van der Jeught, K., Agarwal, P., Zhang, Y., Liu, S., Zhao, G., 2019. Precise targeting of POLR2A as a therapeutic strategy for human triple negative breast cancer. Nat. Nanotechnol. 14, 388–397.
Yu, P., Mathieu, J., Lu, G.W., Gabiatti, N., Alvarez, P.J., 2017. Control of antibiotic-resistant bacteria in activated sludge using polyvalent phages in conjunction with a production host. Environ. Sci. Technol. Lett. 4, 137–142. https://doi.org/10.1021/acs.estlett.7b00045.
Yu, P., Wang, Z., Marcos-Hernandez, M., Zuo, P., Zhang, D., Powell, C., Pan, A.Y., Villagrán, D., Wong, M.S., Alvarez, P.J.J., 2019. Bottom-up biofilm eradication using bacteriophage-loaded magnetic nanocomposites: a computational and experimental study. Environ. Sci. Nano 6, 3539–3550. https://doi.org/10.1039/c9en00827f.
Zhang, X., Yang, H., Wang, X., Karanfil, T., Xie, Y.F., 2015. Trihalomethane hydrolysis in drinking water at elevated temperatures. Water Res. 78, 18–27.
Zhao, Z., Ding, C., Wang, Y., Tan, H., Li, J., 2019. pH-Responsive polymeric nanocarriers for efficient killing of cariogenic bacteria in biofilms. Biomater. Sci. 7, 1643–1651.
Zuo, P., Yu, P., Alvarez, P.J.J., 2021. Aminoglycosides antagonize bacteriophage proliferation, attenuating phage suppression of bacterial growth, biofilm formation, and antibiotic resistance. Appl. Environ. Microbiol. AEM-00468. https://doi.org/10.1128/aem.00468-21.